Pandemic Restrictions in 2020 highlight the significance of non-road NO$_x$ sources in central London

Samuel J. Cliff[1], Will Drysdale[1], James D. Lee[1], Carole Helfter[2], Eiko Nemitz[2], Stefan Metzger[3, 4], and Janet F. Barlow[5]

[1]Wolfson Atmospheric Chemistry Laboratories, Department of Chemistry, University of York, York, YO10 5DD, UK
[2]UK Centre for Ecology and Hydrology, Bush Estate, Penicuik, EH26 0QB, UK
[3]Battelle, National Ecological Observatory Network. 1685 38th Street, Boulder, CO 80301, USA
[4]Dept of Atmospheric and Oceanic Sciences, University of Wisconsin-Madison, 1225 W Dayton St, Madison, WI 53711 USA
[5]Department of Meteorology, University of Reading, Reading, RG6 6BB, UK

Correspondence: Samuel J. Cliff (samcliff1@googlemail.com)

Abstract. Fluxes of nitrogen oxides (NO$_x$ = NO + NO$_2$) and carbon dioxide (CO$_2$) were measured using eddy covariance at the BT Tower in central London during the coronavirus pandemic. Comparing fluxes to those measured in 2017 prior to the pandemic restrictions and the introduction of the Ultra-Low Emissions Zone (ULEZ) highlighted a 75 % reduction in NO$_x$ emissions between the two periods but only a 20 % reduction in CO$_2$ emissions and a 32 % reduction in traffic load.

5 Use of a footprint model and the London Atmospheric Emissions Inventory (LAEI) identified transport and heat and power generation to be the two dominant sources of NO$_x$ and CO$_2$ but with significantly different relative contributions for each species. Application of external constraints on NO$_x$ and CO$_2$ emissions allowed the reductions in the different sources to be untangled identifying that transport NO$_x$ emissions had reduced by > 75 % since 2017. This was attributed in part to the success of air quality policy in central London, but crucially due to the substantial reduction in congestion that resulted from

10 pandemic reduced mobility. Spatial mapping of the fluxes suggests that central London was dominated by point source heat and power generation emissions during the period of reduced mobility. This will have important implications on future air quality policy for NO$_2$ which until now, has been primarily focused on the emissions from diesel exhausts.

1 Introduction

Air pollution is thought to be the world's largest environmental risk to human health causing an estimated 7 million premature

15 deaths every year (World Health Organisation, 2018). One species of pollutants of particular concern, especially in the UK, is NO$_x$. Formed as a by-product of high temperature combustion, NO$_x$ is commonly emitted from the tailpipe exhaust of internal combustion engine vehicles and through the use of fossil fuels to generate heat and energy in the residential, commercial and industrial sectors. The major component of NO$_x$ is nitrogen dioxide (NO$_2$); direct exposure to which is known to contribute to respiratory infections such as bronchitis and pneumonia (Ciencewicki and Jaspers, 2007). Indirectly, NO$_x$ is a key component

20 to the photochemical formation of ozone and fine particulate matter (PM$_{2.5}$). Exposure to ozone and PM$_{2.5}$ have additional adverse effects on the respiratory and cardiovascular systems (Zhang et al., 2019). Consequentially, NO$_2$ and PM$_{2.5}$ were

estimated to cost the UK's National Health Service (NHS) and social care £1.6bn between 2017 and 2025, rising to £5.6bn if diseases with less robust evidence for an association are included (Public Health England, 2018). This has become particularly relevant since the start of the coronavirus pandemic whereby long-term exposure to air pollution has been associated with the severity of COVID-19 cases (Imperial College London, 2021).

In 2008, countries in the EU were set legally binding limits for NO_2 concentrations in line with the World Health Organisation (WHO) recommendations. These are 40 μg m^{-3} for the annual mean with no more than 18 exceedances of the 200 μg m^{-3} hourly limit every year (European Parliament, 2008). This target was expected to be met by 2010. In 2021, the WHO reduced the recommended annual mean limit by 75 % to 10 μg m^{-3}.

London is a megacity in the UK with extensive NO_2 air quality issues. Almost all roadside locations exceeded the European Limit Value for NO_2 every year between 2010 and 2016 (Font et al., 2019). Being in a highly developed position with significant resources, it has acted as a testing bed for policy intervention to try and curb emissions and achieve these air quality targets. These have been focused largely on traffic pollution and congestion charging and have the primary goal of reducing NO_x concentrations via reduced road transport emissions, either through reduced traffic numbers or through reduced average emission per vehicle per unit distance. Most notable is the introduction of the world's first ultra-low emissions zone (ULEZ), launched on 8th April 2019 with the zone spatially shown in Figure 1 a). This operates 24 hours a day, 364 days a year (excludes Christmas Day) and requires a daily payment if the vehicle driven inside the zone does not meet the most stringent emissions standards (currently Euro III for motorbikes, Euro IV for petrol cars and Euro VI for diesel cars and larger vehicles), in addition to the congestion charging payment within the same area. The ULEZ was expanded on 25th October 2021 up to the north and south circular roads in an 18-fold increase in size. In addition to policy, the coronavirus pandemic had significant implications on NO_x emissions in the UK through reduced mobility. During 2020 and 2021 the UK staged three lockdowns with "stay at home" orders. Full details on the timings and the severity of lockdown restrictions in London can be found in Figure A1.

Assessment of the impact of policy intervention and other external stimulus like the coronavirus pandemic on NO_x emissions is crucial for the future design and implementation of air quality policy in the UK. Eddy-covariance is a technique used to quantify the surface atmosphere exchange of an atmospheric pollutant. The calculated flux coupled with a footprint model provides information on surface emissions, allowing for changes to be studied and for direct comparison to the emissions inventories used in policy development. Whilst most frequently used for measuring carbon dioxide exchange with ecosystems from stationary towers (Baldocchi et al., 2001; Griffis et al., 2008; Butterbach-Bahl et al., 2013), the technique has been extended to the urban canopy for both greenhouse gases and air pollutants (Langford et al., 2010; Lee et al., 2014; Helfter et al., 2016; Karl et al., 2017), as well as to airborne measurements for the assessment of fluxes at a much greater spatial extent (Vaughan et al., 2021; Metzger et al., 2013; Vaughan et al., 2017).

Here we present the first year of data from the long-term NO_x flux measurement programme at the BT Tower (London, UK). As the only long-term measurements of NO_x emissions from a megacity in the world this is a highly unique and potentially powerful data-set. The NO_x emissions measurements are combined with additional CO_2 emissions measurements, a

footprint model and the London Atmospheric Emissions Inventory (LAEI) to source apportion changes in emissions due to the coronavirus pandemic and the ULEZ. Resulting policy implications are inferred.

2 Experimental

2.1 Measurement Site

60 Instruments for measuring fluxes of urban air pollutants and greenhouse gases are situated in a small lab atop the British Telecommunications tower (BT Tower) located in central London, UK (51°31'17.4"N, 0°8'20.04"W). The measurement height is 190 m above street level, with a mean building height of 8.8 ± 3.0 m in the 10 km radius surrounding the tower (Lee et al., 2014). The gas inlet and ultrasonic anemometer are attached to a mast that extends 3 m above the top of the tower. Air is pumped down a 45 m Teflon tube (3/8" OD) in a turbulent flow of 20-25 L min^{-1} to the gas instruments, which are situated in 65 a small air conditioned room inside the tower on the 35th floor.
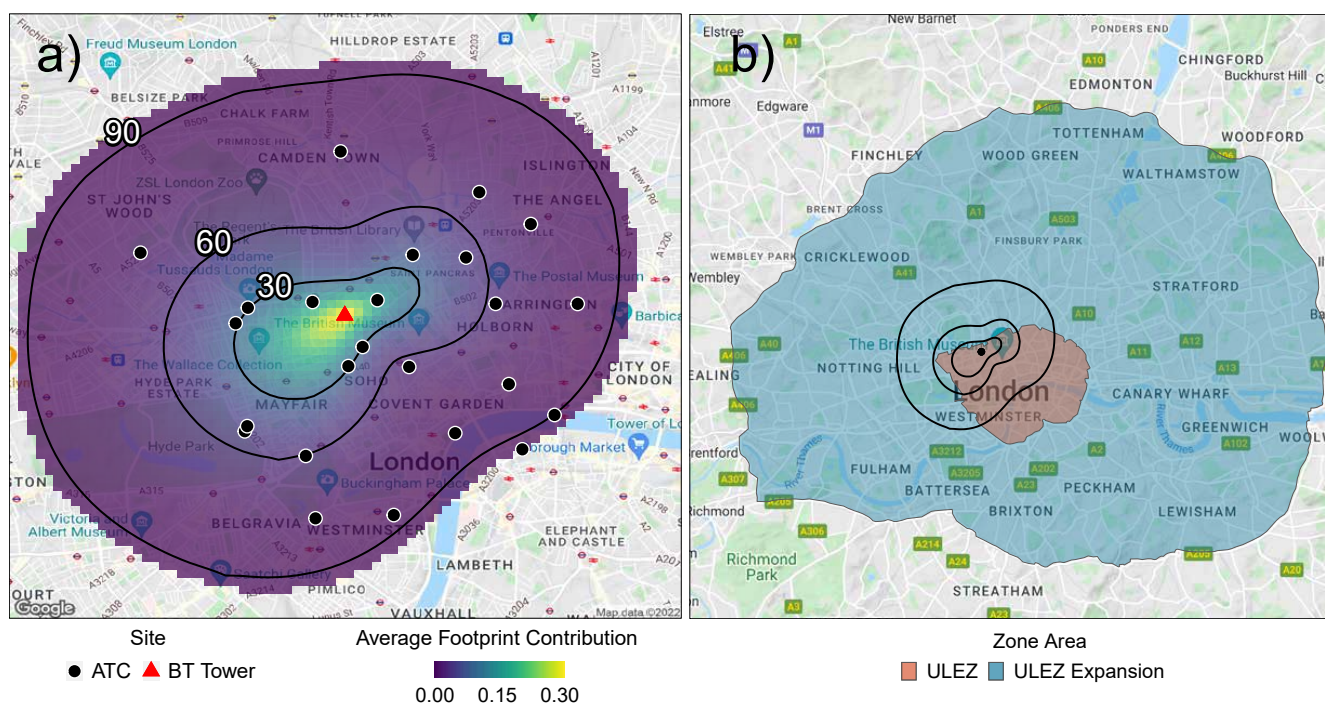
Figure 1. a) The average footprint climatology for the Sept 2020-Sept 2021 time period, with the 30, 60 and 90 % contribution contours and the location of the 24 ATC sites and the BT Tower site overlaid. b) Spatial boundary of the ULEZ (red) and ULEZ expansion (blue) with the same footprint contribution contours presented in a) overlaid as black lines, and the BT Tower site marked as a black dot. Maps produced from Google Maps (© Google Maps 2021) accessed using an API in R.

2.2 NO$_x$ measurements

Long-term measurements of NO and NO$_2$ fluxes began in September 2020 with data presented here up to September 2021. Both chemical species were measured using a dual channel chemiluminescence analyser (Air Quality Design Inc., Boulder Colorado, USA; 5 Hz). The number of photons measured by the photomultiplier tube were converted into a part per trillion 70 (ppt) mixing ratio using a five point calibration curve produced through dilutions of a 5 ppm NO in N$_2$ calibration standard (BOC Ltd., UK; traceable to the scale of the UK National Physical Laboratory, NPL) into NO$_x$ free air. NO$_2$ was calculated by conversion of NO$_2$ into NO using a photolytic blue light converter (BLC). Here, both NO and NO$_2$ were measured, from which NO$_2$ can be quantified by subtracting the NO mixing ratio and applying a correction factor for the conversion efficiency of the BLC. The instrument was calibrated every 37 hours in addition to an hourly zero measurement to subtract the temperature 75 dependent background signal of each channel.

2.3 CO$_2$ measurements

Long-term measurements of CO$_2$ have been ongoing at the BT Tower since 2011 as part of UKCEH's National Capability programme. Dry mass fractions were measured initially using a cavity ringdown spectrometer (Model 1301-f, Picarro Inc., Santa Clara, California, USA; 10 Hz) as described by Helfter et al. (2016). Unfortunately, instrumental failure means data is not 80 available between February and June 2021, after which a closed path infrared gas analyser (Li-7000, LI-COR Environmental, Lincoln, Nebraska, USA; 10 Hz) took over the CO$_2$ flux measurement.

2.4 Meteorological measurements

Meteorological measurements were made at the BT Tower as described by Lane et al. (2013). Wind speed, wind direction and sonic temperature were measured using a ultrasonic anemometer (Gill R3-50, Gill Instruments, Lymington, UK; 20 Hz), along 85 with pressure and relative humidity measurements using a weather station (WXT520, Vaisala Corp. Helsinki, Finland; 1 Hz).

2.5 Flux Calculations

The flux, F, is defined in this context as the vertical transport of a chemical species per unit area per unit time. Hourly fluxes were calculated using eddy covariance theory as described by Eq. (1), where F is equal to the covariance between the instantaneous change in vertical wind speed, w', and the instantaneous change in species concentration, c', averaged over the hour.

90 $$F = \overline{w'c'} \tag{1}$$

Eddy-covariance calculations were performed using the modular software packages in eddy4R adopting the same processing settings described in Drysdale et al. (2022) as adapted from Squires et al. (2020) This was to allow a direct comparison to be made to the previous measurements made in 2017. Data was filtered such that the friction velocity (u*) is > 0.2 to ensure

sufficiently developed turbulence and using eddy4R's quality control flagging scheme based on both a combination of input
95   data validation, stationarity and integrated turbulence characteristics (Metzger et al., 2017; Smith and Metzger, 2013).

2.6   Footprint Modelling

A parameterised version of the backwards Lagrangian stochastic particle dispersion model implemented in eddy4R was used
to estimate the footprint for each hourly flux measurement at the BT Tower. The model is described by Kljun et al. (2004)
and has been parameterised for a range of meteorological conditions and receptor heights to reduce the computational expense
100   of running it. The original model aims to produce a cross-wind integrated footprint function as a function of its along-wind
distance, which has now been further extended into two dimensions using a Gaussian distribution driven by the standard devi-
ation in the cross-wind component (Metzger et al., 2012; Kljun et al., 2015). Meteorology statistics from the eddy covariance
calculations are used in combination with modelled boundary layer height from ERA5 (Copernicus Climate Change Service
Climate Data Store (CDS), 2021), and a surface roughness length of 1.1 m to produce a weighted matrix of 100 m x 100 m
105   grid cells. Each output weighted matrix was then scaled and aligned to an appropriate coordinate reference system to allow
each matrix to be plotted onto a map.

2.7   Traffic Data

Hourly traffic loads surrounding the BT Tower were calculated by summing the traffic load from each of the 24 Automatic
Traffic Counters (ATCs) within the flux footprint, as shown in Figure 1. This gave an indication of the magnitude of traffic
110   load for both measurement periods and allowed relative changes to be studied between the two years. In addition, daily vehicle
length breakdown was examined from which vehicles were separated into three length classes: < 5.2 m, indicating the number
of passenger cars, 5.2 m-12 m, indicating the number of vans and rigid lorries and > 12 m, indicating the number of buses and
arctic lorries. As the LAEI estimates that almost all lorry emissions in central London are due to the rigid class, the >12 m
class is assumed to solely be made up from buses. Data was provided by the Operational Analysis Department, Transport for
115   London (TFL) via a freedom of information request (Transport for London, 2021).

2.8   Emissions inventories

The London Atmospheric Emissions Inventory (LAEI) is a spatially disaggregated 1 km^2 gridded map of the annual emissions
of various air pollutants for the London area up to the M25 motorway ring road (Greater London Authority, 2016). Annual
emissions are estimated using emission factors and activity factors for the different sources. For example, emissions from
120   domestic combustion in (tonnes/year) would be calculated as Gas Consumption (GW.h/year) × Emission Factor (t poll/GW.h).
The inventory is produced roughly every 3 years by TFL and the Greater London Authority (GLA). At the time of writing,
there was no inventory estimates for the pandemic affected years of 2020 and 2021. We therefore use the most recent version
produced in 2016, which relates to a 'normal' year unaffected by lockdowns, to understand how emissions have changed since
the 2017 measurements.
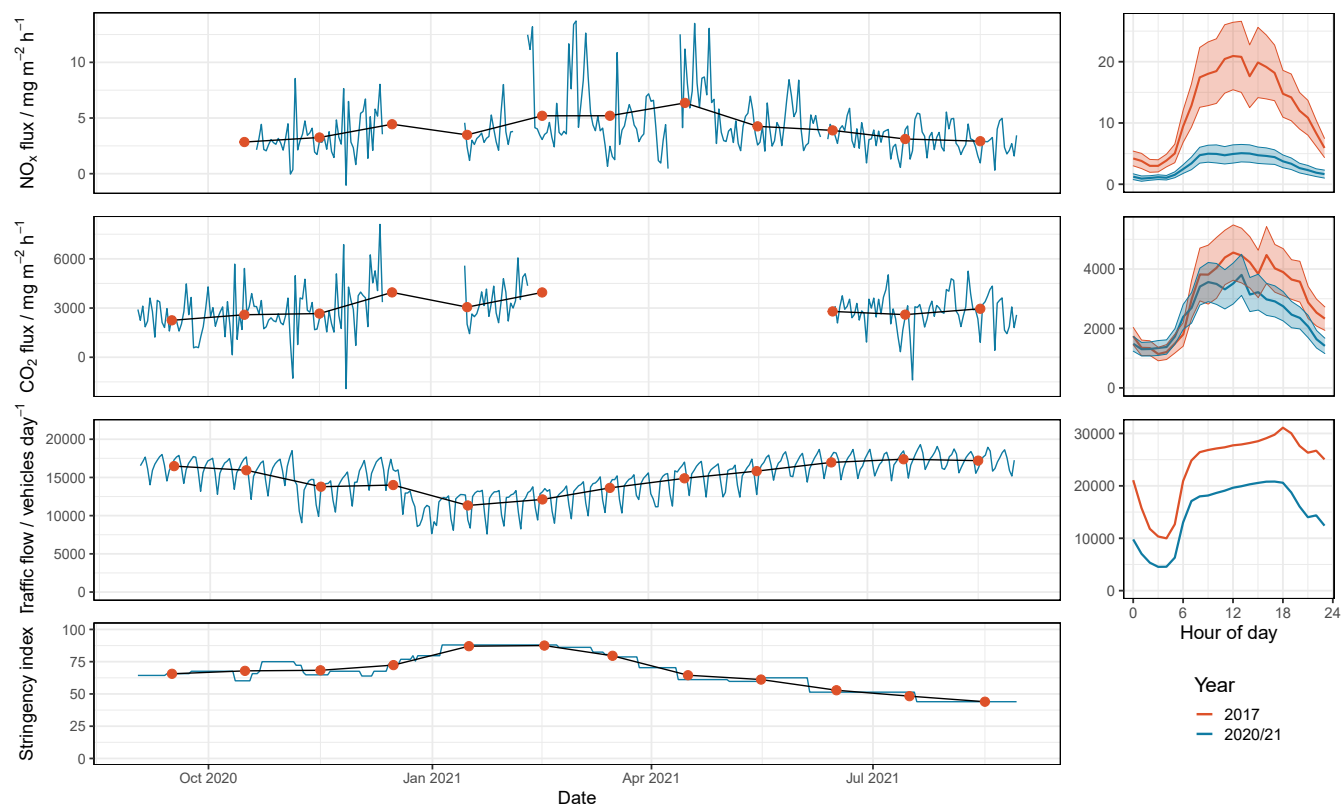
Figure 2. Time series from September 2020 to September 2021 for daily time averaged NO_x flux, CO_2 flux, traffic load around the tower and stringency index in the UK. Also shown are monthly averages for each variable as red dots centered around the center of each month. Average median diurnal profiles with error bars for the data are shown to the right in blue for 2020/21 in comparison to those generated from the 2017 data in red.

Of the 8760 hours in the year, 7034 hours of NO_x fluxes were calculated. Data loss was largely due to instrument or sample pump failure. Of these 7034 hours, a further 1341 were removed by the quality control flagging to leave 5693 hours or 65 % of high-quality fluxes to be analysed. This data is displayed in Figure 2 along with measured CO_2 flux, traffic load around the tower and the UK's restrictions stringency index as calculated by the Oxford COVID-19 Government Response Tracker (Hale

130 et al., 2021). Traffic load around the tower was strongly anti-correlated with stringency index as expected. However, there was no obvious correlation of NO_x flux with traffic load. In fact the highest NO_x emissions were observed when the traffic load was at its lowest, providing a first indication that traffic might not be the dominant source in central London. Traffic loads had not recovered to pre-pandemic levels either (Figure A3) despite the fact all lockdown restrictions were fully removed on 21 June 2021, hinting at a more long-term change in behaviour. This is not unexpected as the stringency index remained at 40

135 %, mainly due to self-isolation requirements and international travel restrictions which were still present at this stage. Study of the average diurnal profiles for each of NO_x flux, CO_2 flux and traffic load around the tower in Figure 2 for this data, and the 2017 data described by Drysdale et al. (2022), highlighted an 75 % reduction in NO_x flux since 2017. However, only a corresponding 20 % reduction in CO_2 flux and 32 % reduction in traffic load was observed.

3.1 Calculation of inventory estimated emissions

140 Estimated emissions from the London Atmospheric Emissions Inventory (LAEI) for the measurement footprint were calculated to aid understanding of these observations. The hourly footprint weighted matrix output from eddy4R was used to select the relevant areas of the LAEI. The theoretical contribution to the flux was extracted from each footprint grid cell and scaled for hour of day, day of week and month of year for each emissions sector using a set of anthropogenic scaling factors described by Drysdale et al. (2022). An excellent agreement between the diurnal profiles and measurement footprint (shown in Figure

145 A2) for the 2017 and 2020/21 measurement periods was seen. This gave us confidence that any changes in emissions were not to do with sampling in different times of year or sampling in different areas of central London. The source breakdown of the 2017 inventory generated time series for both CO_2 and NO_x is shown in Figure 3. Emissions of both species are almost entirely made up from combustion of fossil fuels to generate heat and power in the domestic, commercial and industrial sectors and the transport sector, which is dominated by various forms of road transport. However, each species has a significantly different

150 relative contribution from each sector. 75 % of CO_2 emissions are estimated to arise from heat and power generation but only 42 % of NO_x emissions from the same source.

3.2 Source apportionment of emissions reduction

The inventory breakdown for each species and the different percentage reductions in measured emissions since 2017 were used to disentangle changes in emissions of each sector. This was done simultaneously using a number of assumptions.

Table 1. A summary of the data used in the formation of simultaneous Eqs. (2) and (3).

	NO_x	CO_2
% measured reduction in emissions since 2017	75 %	20 %
% contribution from heat and power generation	0-50 % (α)	75 %
% contribution from transport	50-100 % (β)	25 %
% reduction in heat and power generation emissions	x	x
% reduction in transport emissions	y'	y

155 Helfter et al. (2016) highlight the excellent agreement of CO_2 emissions measured at the BT Tower to those estimated by the LAEI and thus the source contributions of 75 % from heat and power generation and 25 % from transport for CO_2 are taken as accurate here. On the other hand, previous observations have shown a significant underestimation of NO_x emissions in central London. This is most likely due to an underrepresentation of road transport NO_x emissions in line with a poor
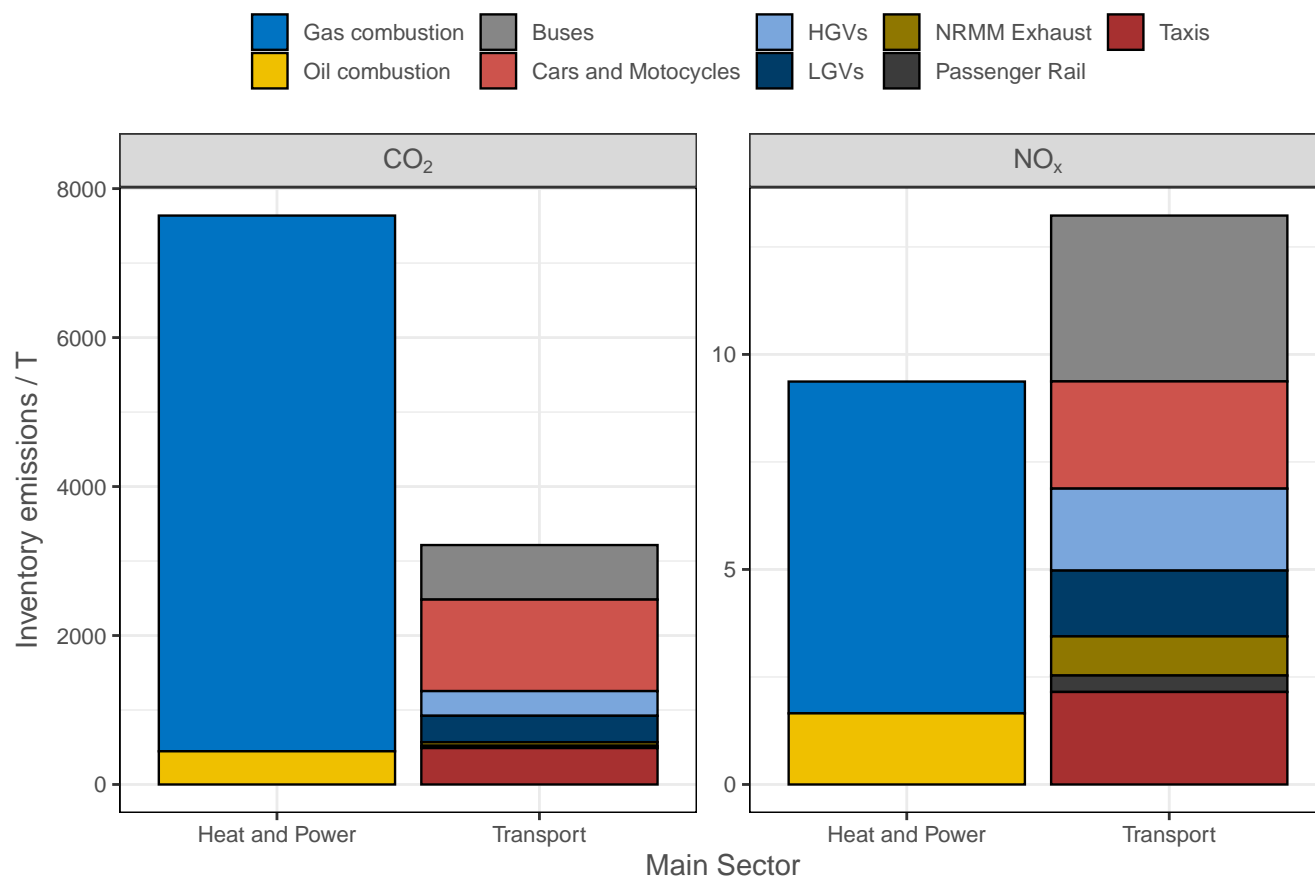
Figure 3. Inventory estimated breakdown of emissions for CO_2 (left) and NO_x (right) in Tonnes for March through August of 2017 as determined from the inventory emissions extraction for our hourly measurement footprint. LGV = Light Goods Vehicles, HGV = Heavy Goods Vehicles, NRMM = Non-Road Mobile Machinery.

representation of diesel vehicle emissions and/or congestion. Therefore, rather than using the inventory predicted 42:58 split
160 for heat and power generation:transport the relative contributions were varied. Labelled as $\alpha : \beta$, different scenarios between
50:50 and 0:100 (where $\alpha + \beta = 100\%$) were chosen to represent all possible levels of NO_x underestimation. The percentage
reduction in heat and power generation emissions for both species is labelled as x with the assumption that any reduction in this
sector's emissions would have the same reduction in measured flux for both species. With minimal legislation for the sector
introduced between 2017 and 2020/21 and a failure to address NO_x emissions from boilers in the UK's Clean Air Strategy,
165 this assumption is considered reasonable. However, this is is likely to be untrue for transport. Policy implemented between
the two measurement periods specifically targeted NO_x emissions and NO_x emissions are disproportionately higher in higher
traffic loads due to the ineffectiveness of exhaust treatment systems in that environment. Additionally, the modernisation of
the vehicle fleet will have introduced more vehicles with lower NO_x/CO_2 emission ratios. Therefore, the relative change in the

emissions of NO_x and CO_2 from traffic sources may not have been the same, and different values are given here as y and y'.
170 This information is all summarised in Table 1 with the two independent constraints displayed in Eq.'s (2) for CO_2 and (3) for NO_x:

$$\delta CO_2 = 0.75x + 0.25y_{[32,100]} = 20\% \tag{2}$$

$$\delta NO_x = \alpha x + \beta y'_{[75,100]} = 75\% \tag{3}$$

The different scenarios are visualised in Figure 4 to aid understanding of the possible solutions. Two bounding conditions
175 drawn as hashed lines are applied to constrain the solutions. These are as follows: a) A reduction in transport emissions greater
than 100 % is not possible and b) CO_2 emissions from transport must have decreased by at least 32 % in line with the 32 %
reduction in traffic load. Highlighted in green are all the resulting possible solutions where crucially, to achieve the observed
reductions in NO_x flux, there must have been a 75-100 % reduction in transport NO_x emissions with transport contributing
> 70 % to total NO_x emissions. This transport contribution percentage demonstrates the underestimation in the inventory of
180 transport emissions in agreement with Karl et al. (2017) and Drysdale et al. (2022). However, the most interesting observation
is that a 75-100 % decrease in transport NO_x emissions is seen for only a 32 % decrease in traffic load since 2017.

When compared to concentrations, we found that NO_x concentrations at Marylebone Road, a kerbside monitoring site within
the flux footprint, had declined by 62 % between the two periods (248 vs 95 μg m^{-3}). This is increased to 69 % (214 vs 67 μg
m^{-3}) when looking at the roadside increment concentration (roadside – urban background) as determined from Marylebone
185 Road and London North Kensington monitoring sites. Whilst this was slightly lower in magnitude than the measured change in
flux, the concentration data will have been heavily influenced by meteorology and so some disagreement was expected. There
are a number of plausible explanations for the large decrease in NO_x fluxes. The introduction of the ULEZ is thought to have
resulted in a pre-pandemic 31 % reduction in NO_x emissions from road transport in central London (Greater London Authority,
2020); this is likely to be an upper estimate for our measurements due to the fact a significant proportion of our flux footprint
190 being situated outside of the ULEZ zone. With average traffic loads between April and November 2019 after the ULEZ was
introduced only down 1.8 % on 2018 levels for the same period, the vast majority of the reduction is due to a clean-up of the
fleet which reduces the emissions per vehicle per unit distance. The remaining emissions are further reduced by 32 % due there
being 32 % less vehicles on the roads surrounding the BT tower during the pandemic. This leaves 22-47 % of unaccounted
for emissions reduction. A small portion of this unaccounted for reduction may be due to a 40 % reduction in the number of
195 buses on the roads surrounding the BT Tower during 2020/21. The >12 m class of the vehicle length breakdown in Figure A4
represents the bus classification. With buses making up 17 % of the total NO_x emissions from road transport, the decrease in
relative proportion between 2017 and 2020/21 could result in a maximum of 7 % extra reduction in NO_x emissions. It is likely
to be less than 7 % due to the small increase in the relative proportion of the 5.2 m-12 m class.
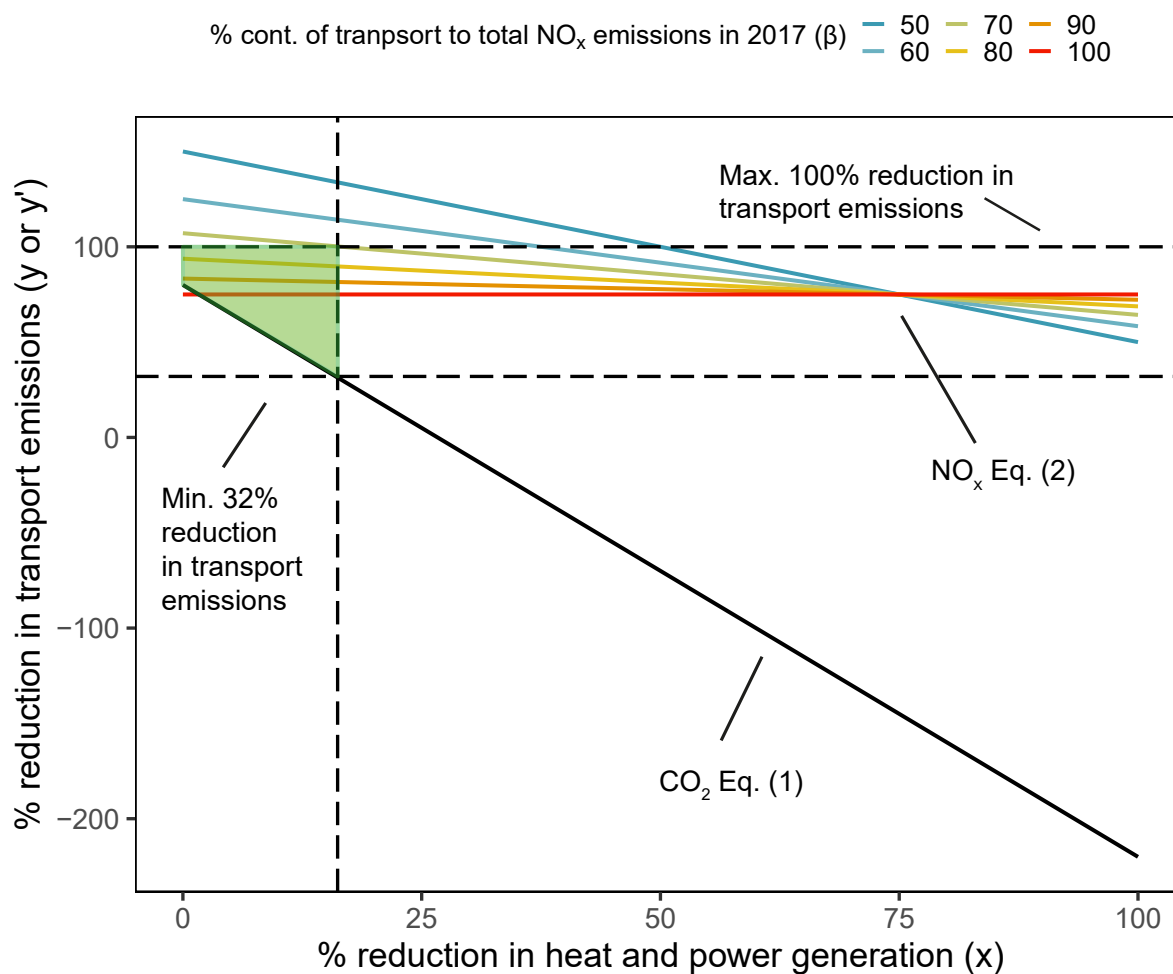
Figure 4. A plot showing the external constraints on NO_x and CO_2 emissions. Eq. (2) is shown as the solid black line and Eq. (3) as the coloured solid lines, with each colour reflecting a different value of β. The two horizontal hashed lines represent the two discussed constraints, and the vertical hashed line shows the constraint the minimum of 32 % reduction in traffic CO_2 emissions has on the NO_x scenarios. All possible solutions when the constraints are applied are highlighted by the shaded green area.

3.3 Flux correlations with traffic load

200 Examining how the NO_x flux correlated with traffic load for both measurement time periods gives further insight into the un-accounted emissions reduction. Figure 5 generally shows significantly enhanced NO_x emissions in 2017 above 25000 vehicles hr^{-1}. With road transport being the dominant source during these measurements it is highlighting what is thought to be the effect of congestion on NO_x emissions.
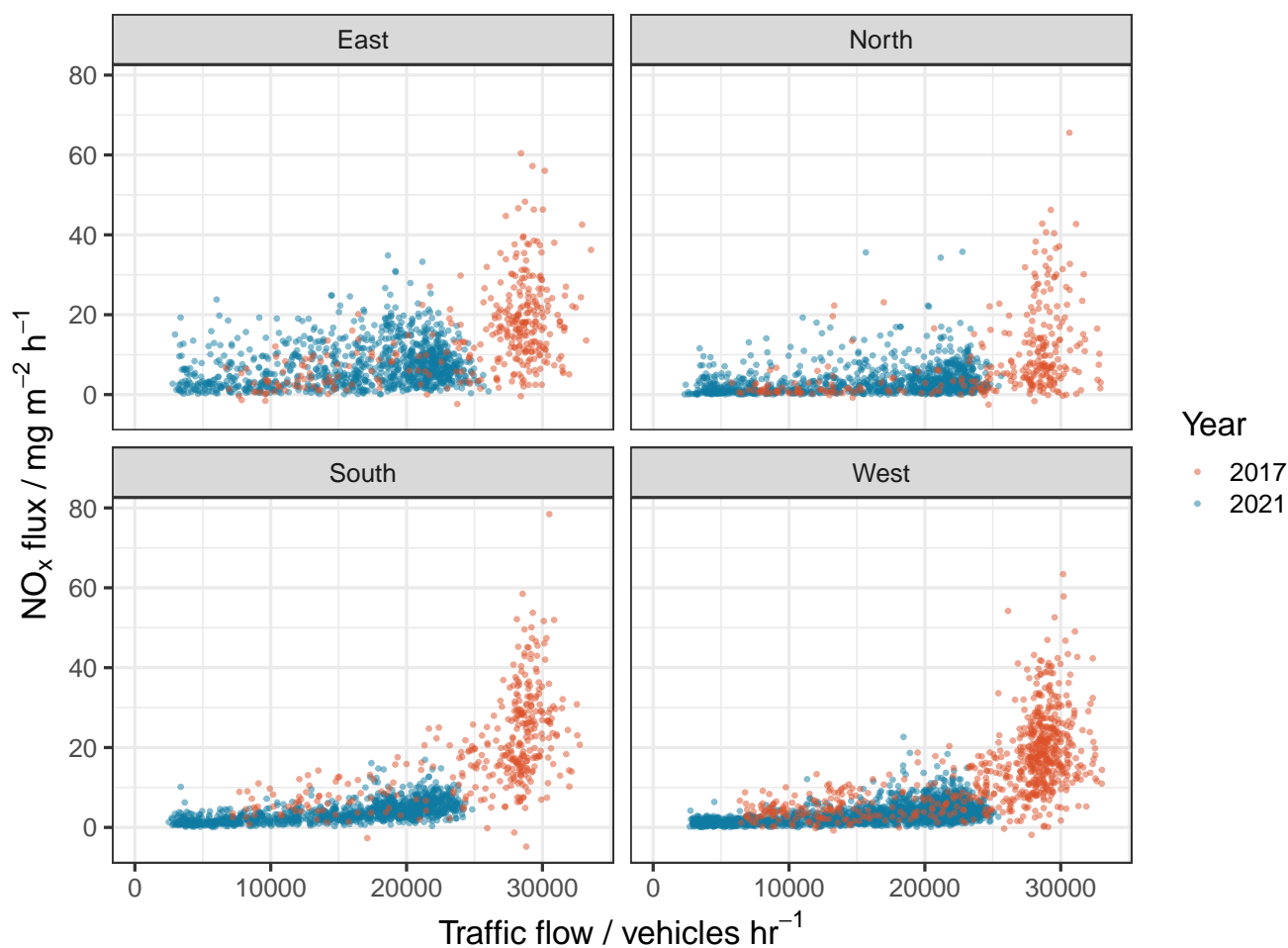
Figure 5. Comparison of the measured NO_x flux with hourly traffic load (sum of the 24 surrounding ATCs) for March through August 2017 (red) and March through August 2021 (blue), both inclusive. The data is split by wind direction: North (315°-45°), east (45°-135°), south (135°-225°) and west (225°-315°).

During periods of high congestion, increased emissions are expected due to increased length in journey time, a greater
205 number of accelerations in the stop start nature of traffic and reduced effectiveness of exhaust gas NO_x treatment systems in diesel vehicles at low engine temperatures (Carslaw and Rhys-Tyler, 2013). The effect of congestion on NO_x emissions is

highly dependent on several variables including the fleet composition, type of exhaust treatment system and the actual level of congestion (Ko et al., 2019). It is thought that for individual roads, excess emissions from congestion can be anything up to 75 % greater than non-congested roads (Gately et al., 2017). Therefore, it is thought that reducing the peak traffic load

210 below 25000 vehicles hr^{-1} has had a large impact on traffic NO$_x$ emissions, more than accounting for the remaining emissions reduction.

3.4 Spatial Mapping

This change in emissions is clearly seen in the spatial mapping of the NO$_x$ fluxes in Figure 6. Drysdale et al. (2022) assigned the heightened emissions to the northeast of the BT Tower in Figure 6 a) to Euston station, including not only the train station,

215 but also the large Euston bus station, taxi ranks and busy roads feeding the station. In addition, the high fluxes measured to the southwest are assigned to highly congested streets such as Oxford Street, Regent Street and Piccadilly. Both areas are associated with high traffic volumes and congestion and support the notion that road transport emissions dominate in central London in 2017. However, these areas have almost an order of magnitude smaller emissions and are barely visible for 2020/21 when shown on the same scale. This adds additional support to the conclusion that reduced traffic load and thus congestion in

220 2020/21 have been a major cause of the reduced NO$_x$ flux.

The spatial map for 2020/21 in Figure 6 c) on its own scale identified a shift in the dominant NO$_x$ emissions source between 2017 and 2020/21. Whilst Euston station and the previously congested southwesterly area are still noticeable, the major stand out area is to the east. Depicted as a white box is the outline of the University of London point source as documented by the National Atmospheric Emissions Inventory, a similar inventory to the LAEI but for the whole of the UK (Defra and BEIS).

225 The University of London is the largest university in the UK and its Bloomsbury Campus appears directly under the heightened emissions area. This site is made up of much of the University College London (UCL) central administration, the UCL hospital and Bloomsbury Heat and Power, a number of combined heat and power (CHP) sites to power the university. CHP systems simultaneously generate heat and electrical power from a single source of energy. By capturing and utilising the heat that is generated as a by product of the electricity generation process, efficiency is increased which can reduce carbon emissions by

230 up to 30 % compared to conventional separate generation (Department for Business, Energy and Industrial Strategy (BEIS), 2021). However, the requirement for CHP to be in urban areas risks an increase in air pollution. Indeed it has been shown that CHP can "substantially" impact air quality due to NO$_x$, the highest criteria judged by Environment Protection UK and the Institute of Air Quality Management (Kings College London, 2018). Here, the heat and power generation source stands out and dominates over transport but is only seen due to the drastic reduction in transport NO$_x$ emissions during the period of

235 pandemic reduced mobility. The greatly reduced correlation with traffic load for the easterly 2020/21 data in Figure 5 is further evidence that the dominant source in this direction is heat and power generation.
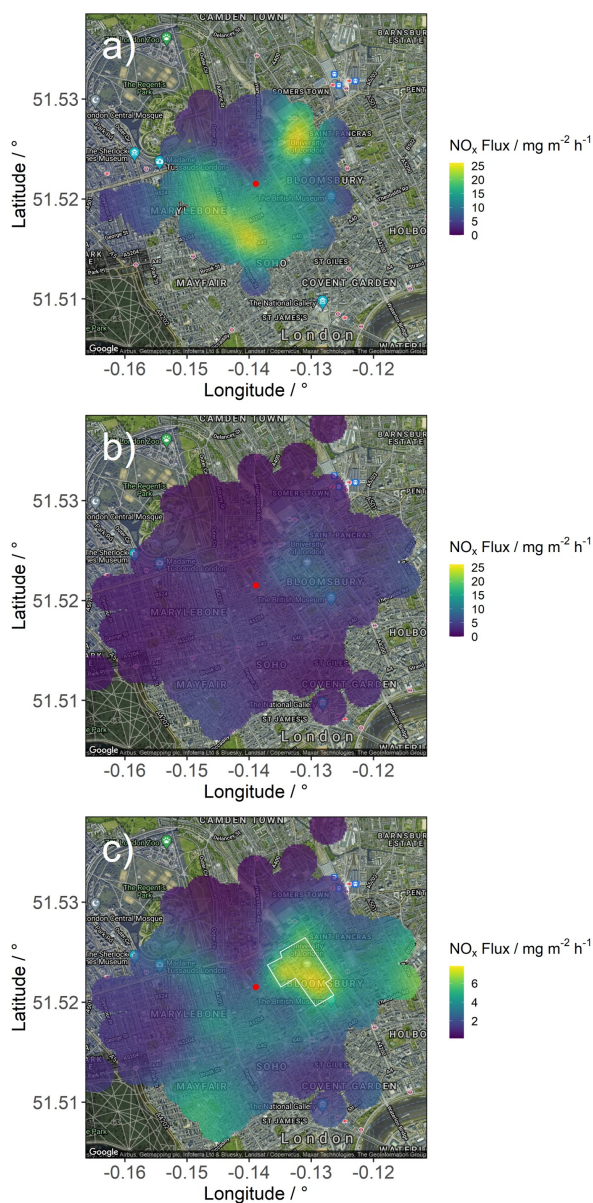
Figure 6. NO$_x$ flux surfaces as a function of along-wind distance to the footprint maximum contribution and wind direction, as derived by Drysdale et al. (2022), for a) March through August 2017 and b) September 2020 to September 2021, displayed on the same scale for ease of visual comparison. Also shown in c) September 2020 to September 2021 on it's own scale with the border for the University of London overlaid in white. The location of the BT Tower site is displayed as a red dot in each spatial map. Maps are produced using Google Maps (© Google Maps 2021) accessed using an API in R.

4   Conclusions

Eddy covariance emissions measurements at the unique BT Tower site in central London provide an opportunity to study the evolution of air pollutant emissions in a megacity and the part that policy and other external stimuli play in improving air quality. Here, the direct emissions measurements have shown that reducing congestion could be an even more effective way of reducing NO_x emissions from road transport than the ULEZ. However, this is not the direction in which the UK is heading. With much cheaper mileage, the continued uptake of electric vehicles is predicted to increase congestion. Reducing the number of vehicles on the road by improving infrastructure for other greener methods of travel such as cycling would not only achieve reduced congestion but give additional benefits to health further reducing costs of treatment at health services (Fishman et al., 2015). A more targeted approach to simultaneously reduce congestion as well as emissions per vehicle per unit distance is therefore recommended to other cities looking to implement policies to tackle high traffic NO_x emissions.

The observation that NO_x emissions in central London during this continuing period of reduced mobility were thought to be dominated by heat and power generation is an important one. This is a transition which was expected to occur in the coming years but was brought forward in time by the pandemic, providing a glimpse into future air quality. As of 2020, there were 2659 CHP sites in the UK with additional widespread usage in Europe (Department for Business, Energy and Industrial Strategy (BEIS), 2021). Due to their increased efficiency and the push towards NetZero economies, they are expected to increase in popularity. Despite this period of drastically reduced transport emissions, all air quality monitoring sites (urban background, urban traffic and curbside) in London far exceeded the new WHO NO_2 air quality target. To achieve these targets it is therefore clear that legislation is required to reduce NO_x emissions from heat and power generation. The heat and power generation source has been somewhat neglected due to the prominence of issues with diesel vehicle emissions. But with the planned use of hydrogen combustion in decarbonisation, which currently has major uncertainties due to a lack of experimental data, now is the critical time to start thinking about policy intervention for this sector (Lewis, 2021). This makes the lack of acknowledgement for gas combustion in boilers in the UK clean air strategy highly disappointing. This is the first indication from a megacity which shows heat and power emissions will need to be regulated to achieve the new air quality NO_x targets. As more and more of the world's population is expected to live in urban areas, it is essential that compliance with WHO targets is achieved to minimise health and economic impacts. The conclusions derived from this work will therefore be of interest to other nations, especially with air quality improvements being increasingly sought in the developing world.

Code availability. The eddy4R v.0.2.0 software framework used to generate eddy-covariance flux estimates can be freely accessed at https://github.com/NEONScience/eddy4R. The eddy4R turbulence v0.0.16 and Environmental Response Functions v0.0.5 software modules for advanced airborne data processing were accessed under Terms of Use for this study (https://www.eol.ucar.edu/content/cheesehead-code-policy-appendix) and are available upon request.

Data availability. Automatic Urban and Rural Network data used in the analysis was obtained from https://uk-air.defra.gov.uk/networks/network-info?view=aurn under "Open Government Licence v3.0" (last access: August 2022). The London Atmospheric Emissions Inventory is available at https://naei.beis.gov.uk/ (© Crown 2022 copyright Defra & BEIS, licenced under the Open Government Licence (OGL)). For the
270   measurement data in this paper, the calculated fluxes are not available in any repository due to the intensity of the processing and interpretation required. We are happy to make this available upon request. 15 min aggregated concentrations are available on the Centre for Environmental Data Analysis database, but these were not directly used here. The ERA5 boundary layer height data can be accessed at http://cds.climate.copernicus.eu/cdsapp#!/home (Copernicus Climate Change Service Climate Data Store (CDS), 2017). The traffic count data used in this article were provided by Transport for London (2021) (Automatic Traffic Counter data; original source data provided by
275   Operational Analysis department, Transport for London).

Author contributions. SJC made the NO_x measurements, calculated the fluxes and performed the analyses. SJC wrote the paper and produced the figures with input from co-authors. WSD provided support with the measurements, flux calculations and interpretation of the data. JDL provided support for the measurements and interpretation of the data. CH and EN provided supporting measurements from the site and aided in interpretation of the data. SM provided training on the eddy4R software and aided in interpretation of the data. JFB provided
280   meteorological data for the site.

Competing interests. The authors declare no competing interest.

Acknowledgements. Measurements were funded by the UK Natural Environment Research Council through the OSCA (Integrated Research Observation System for Clean Air) project of the Clean Air Strategic Priority Fund (Grant numbers NE/T001917/1 and NE/T001798/2) and through award number NE/R016429/1 to UKCEH as part of the UK-SCAPE programme delivering National Capability. Samuel
285   Cliff was supported by the Panorama Natural Environment Research Council (NERC) Doctoral Training Partnership (DTP), under grant NE/S007458/1. The National Ecological Observatory Network is a program sponsored by the National Science Foundation and operated under cooperative agreement by Battelle. This material is based in part upon work supported by the National Science Foundation through the NEON Program. The author also thanks Neil Mullinger and Karen Yeung (UK Center for Ecology and Hydrology) for instrument and sample line maintenance, Ally Lewis and Rhianna Evans for help in manuscript preparation and British Telecom (BT) for granting use of the
290   tall tower for research purposes, in particular Karen Ahern and Guille Parada for arranging work permits and facilitating access to the site.

References

Baldocchi, D., Falge, E., Gu, L., Olson, R., Hollinger, D., Running, S., Anthoni, P., Bernhofer, C., Davis, K., Evans, R., Fuentes, J., Goldstein, A., Katul, G., Law, B., Lee, X., Malhi, Y., Meyers, T., Munger, W., Oechel, W., U, K. T. P., Pilegaard, K., Schmid, H. P., Valentini, R., Verma, S., Vesala, T., Wilson, K., and Wofsy, S.: FLUXNET: A new tool to study the temporal and spatial variability of ecosystem-scale carbon dioxide, water vapor, and energy flux densities, Bulletin of the American Meteorological Society, 82, 2415 – 2434, https://doi.org/10.1175/1520-0477(2001)082<2415:FANTTS>2.3.CO;2, 2001.

Butterbach-Bahl, K., Baggs, E. M., Dannenmann, M., Kiese, R., and Zechmeister-Boltenstern, S.: Nitrous oxide emissions from soils: how well do we understand the processes and their controls?, Philosophical Transactions of the Royal Society B: Biological Sciences, 368, 20130 122, https://doi.org/10.1098/rstb.2013.0122, 2013.

Carslaw, D. C. and Rhys-Tyler, G.: New insights from comprehensive on-road measurements of NO_x, NO_2 and NH_3 from vehicle emission remote sensing in London, UK, Atmospheric Environment, 81, 339–347, https://doi.org/10.1016/j.atmosenv.2013.09.026, 2013.

Ciencewicki, J. and Jaspers, I.: Air Pollution and Respiratory Viral Infection, Inhalation Toxicology, 19, 1135–1146, https://doi.org/10.1080/08958370701665434, 2007.

Copernicus Climate Change Service Climate Data Store (CDS): Copernicus Climate Change Service (C3S): ERA5: Fifth generation of ECMWF atmospheric reanalyses of the global climate.,
https://cds.climate.copernicus.eu/cdsapp#!/home, accessed October 2021, 2021.

Defra and BEIS: National Atmospheric Emissions Inventory, licenced under the Open Government Licence (OGL), Crown Copyright 2020.

Department for Business, Energy and Industrial Strategy (BEIS): Digest of UK Energy Statistics, 2021.

Drysdale, W. S., Vaughan, A. R., Squires, F. A., Cliff, S. J., Metzger, S., Durden, D., Pingintha-Durden, N., Helfter, C., Nemitz, E., Grimmond, C. S. B., Barlow, J., Beevers, S., Stewart, G., Dajnak, D., Purvis, R. M., and Lee, J. D.: Eddy covariance measurements highlight sources of nitrogen oxide emissions missing from inventories for central London, Atmospheric Chemistry and Physics, 22, 9413–9433, https://doi.org/10.5194/acp-22-9413-2022, 2022.

European Parliament: Directive 2008/50/EC of the European Parliament and of the council of 21 May 2008 on ambient air quality and cleaner air for Europe,
https://eur-lex.europa.eu/legal-content/EN/TXT/?uri=CELEX:02008L0050-20150918, accessed October 2022, 2008.

Fishman, E., Schepers, P., and Kamphuis, C. B. M.: Dutch cycling: Quantifying the health and related economic benefits, American Journal of Public Health, 105, e13–e15, https://doi.org/10.2105/AJPH.2015.302724, 2015.

Font, A., Guiseppin, L., Blangiardo, M., Ghersi, V., and Fuller, G. W.: A tale of two cities: is air pollution improving in Paris and London?, Environmental Pollution, 249, 1–12, https://doi.org/10.1016/j.envpol.2019.01.040, 2019.

Gately, C. K., Hutyra, L. R., Peterson, S., and Sue Wing, I.: Urban emissions hotspots: Quantifying vehicle congestion and air pollution using mobile phone GPS data, Environmental Pollution, 229, 496–504, https://doi.org/10.1016/j.envpol.2017.05.091, 2017.

Greater London Authority: London Atmospheric Emissions Inventory 2016, licensed under the Open Government Licence (OGL) v2.0, Crown Copyright 2020, https://data.london.gov.uk/dataset/london-atmospheric-emissions-inventory--laei--2016, accessed March 2022, 2016.

Greater London Authority: Central London ultra low emission zone - ten month report, 2020.

Griffis, T. J., Sargent, S. D., Baker, J. M., Lee, X., Tanner, B. D., Greene, J., Swiatek, E., and Billmark, K.: Direct measurement of biosphere-atmosphere isotopic CO_2 exchange using the eddy covariance technique, Journal of Geophysical Research: Atmospheres, 113, D08 304, https://doi.org/10.1029/2007JD009297, 2008.

Hale, T., Angrist, N., Goldszmidt, R., Kira, B., Petherick, A., Phillips, T., Webster, S., Cameron-Blake, E., Hallas, L., Majumdar, S., and
330   Tatlow, H.: A global panel database of pandemic policies (Oxford COVID-19 Government Response Tracker), Nature Human Behaviour, 5, 529–538, https://doi.org/10.1038/s41562-021-01079-8, 2021.

Helfter, C., Tremper, A. H., Halios, C. H., Kotthaus, S., Bjorkegren, A., Grimmond, C. S. B., Barlow, J. F., and Nemitz, E.: Spatial and temporal variability of urban fluxes of methane, carbon monoxide and carbon dioxide above London, UK, Atmospheric Chemistry and Physics, 16, 10 543–10 557, https://doi.org/10.5194/acp-16-10543-2016, 2016.

335   Imperial College London: Investigating links between air pollution, COVID-19 and lower respiratory infectious diseases, 2021.

Karl, T., Graus, M., Striednig, M., Lamprecht, C., Hammerle, A., Wohlfahrt, G., Held, A., von der Heyden, L., Deventer, M. J., Krismer, A., Haun, C., Feichter, R., and Lee, J.: Urban eddy covariance measurements reveal significant missing NO_x emissions in central Europe, Scientific Reports, 7, 2536–2545, https://doi.org/10.1038/s41598-017-02699-9, 2017.

Kings College London: Urban air pollution from combined heat and power plants, 2018.

340   Kljun, N., Calanca, P., and Rotach, M. W.: A Simple Parameterisation for Flux Footprint Predictions, Boundary-Layer Meteorology, 112, 503–523, https://doi.org/10.1023/B:BOUN.0000030653.71031.96, 2004.

Kljun, N., Calanca, P., Rotach, M. W., and Schmid, H. P.: A simple two-dimensional parameterisation for Flux Footprint Prediction (FFP), Geoscientific Model Development, 8, 3695–3713, https://doi.org/10.5194/gmd-8-3695-2015, 2015.

Ko, J., Myung, C.-L., and Park, S.: Impacts of ambient temperature, DPF regeneration, and traffic congestion on NO_x emissions from
345   a Euro 6-compliant diesel vehicle equipped with an LNT under real-world driving conditions, Atmospheric Environment, 200, 1–14, https://doi.org/10.1016/j.atmosenv.2018.11.029, 2019.

Lane, S., Barlow, J., and Wood, C.: An assessment of a three-beam Doppler lidar wind profiling method for use in urban areas, Environmental Science & Technology, 49, 53–59, https://doi.org/10.1016/j.jweia.2013.05.010, 2013.

Langford, B., Nemitz, E., House, E., Phillips, G. J., Famulari, D., Davison, B., Hopkins, J. R., Lewis, A. C., and Hewitt, C. N.: Fluxes
350   and concentrations of volatile organic compounds above central London, UK, Atmospheric Chemistry and Physics, 10, 627–645, https://doi.org/10.5194/acp-10-627-2010, 2010.

Lee, J. D., Helfter, C., Purvis, R. M., Beevers, S., Carslaw, D. C., Lewis, A. C., Moller, S. J., Tremper, A., Vaughan, A., and Nemitz, E. G.: Measurement of NO_x fluxes from a tall tower in central London, UK and comparison with emissions inventories, Journal of Wind Engineering and Industrial Aerodynamics, 49, 1025–1034, https://doi.org/10.1021/es5049072, 2014.

355   Lewis, A. C.: Optimising air quality co-benefits in a hydrogen economy: a case for hydrogen-specific standards for NO_x emissions, Environ. Sci.: Atmos., 1, 201–207, https://doi.org/10.1039/D1EA00037C, 2021.

Metzger, S., Junkermann, W., Mauder, M., Beyrich, F., Butterbach-Bahl, K., Schmid, H. P., and Foken, T.: Eddy-covariance flux measurements with a weight-shift microlight aircraft, Atmospheric Measurement Techniques, 5, 1699–1717, https://doi.org/10.5194/amt-5-1699-2012, 2012.

360   Metzger, S., Junkermann, W., Mauder, M., Butterbach-Bahl, K., Trancón y Widemann, B., Neidl, F., Schäfer, K., Wieneke, S., Zheng, X. H., Schmid, H. P., and Foken, T.: Spatially explicit regionalization of airborne flux measurements using environmental response functions, Biogeosciences, 10, 2193–2217, https://doi.org/10.5194/bg-10-2193-2013, 2013.

Metzger, S., Durden, D., Sturtevant, C., Luo, H., Pingintha-Durden, N., Sachs, T., Serafimovich, A., Hartmann, J., Li, J., Xu, K., and Desai, A. R.: eddy4R 0.2.0: a DevOps model for community-extensible processing and analysis of eddy-covariance data based on R, Git, Docker, and HDF5, Geoscientific Model Development, 10, 3189–3206, https://doi.org/10.5194/gmd-10-3189-2017, 2017.

Public Health England: Estimation of costs to the NHS and social care due to the health impacts of air pollution: summary report, 2018.

Smith, D. and Metzger, S.: Algorithm Theoretical Basis Document: Quality Flags and Quality Metrics for TIS Data Products, https://data.neonscience.org/api/v0/documents/NEON.DOC.001113vA, accessed June 2022, 2013.

Squires, F. A., Nemitz, E., Langford, B., Wild, O., Drysdale, W. S., Acton, W. J. F., Fu, P., Grimmond, C. S. B., Hamilton, J. F., Hewitt, C. N., Hollaway, M., Kotthaus, S., Lee, J., Metzger, S., Pingintha-Durden, N., Shaw, M., Vaughan, A. R., Wang, X., Wu, R., Zhang, Q., and Zhang, Y.: Measurements of traffic-dominated pollutant emissions in a Chinese megacity, Atmospheric Chemistry and Physics, 20, 8737–8761, https://doi.org/10.5194/acp-20-8737-2020, 2020.

Transport for London: Transport for London: original source data provided by Operational Analysis department, 2021.

Vaughan, A. R., Lee, J. D., Shaw, M. D., Misztal, P. K., Metzger, S., Vieno, M., Davison, B., Karl, T. G., Carpenter, L. J., Lewis, A. C., Purvis, R. M., Goldstein, A. H., and Hewitt, C. N.: VOC emission rates over London and South East England obtained by airborne eddy covariance, Faraday Discuss., 200, 599–620, https://doi.org/10.1039/C7FD00002B, 2017.

Vaughan, A. R., Lee, J. D., Metzger, S., Durden, D., Lewis, A. C., Shaw, M. D., Drysdale, W. S., Purvis, R. M., Davison, B., and Hewitt, C. N.: Spatially and temporally resolved measurements of NO_x fluxes by airborne eddy-covariance over Greater London, Atmospheric Chemistry and Physics Discussions, 2021, 1–27, https://doi.org/10.5194/acp-21-15283-2021, 2021.

World Health Organisation: Global health estimates 2016: deaths by cause, age, sex, by country and by region, 2000–2016., https://www.who.int/health-topics/air-pollution#tab=tab_1, accessed October 2021, 2018.

Zhang, J., Wei, Y., and Fang, Z.: Ozone pollution: A major health hazard worldwide, Frontiers in Immunology, 10, 2518, https://doi.org/10.3389/fimmu.2019.02518, 2019.

Appendix A
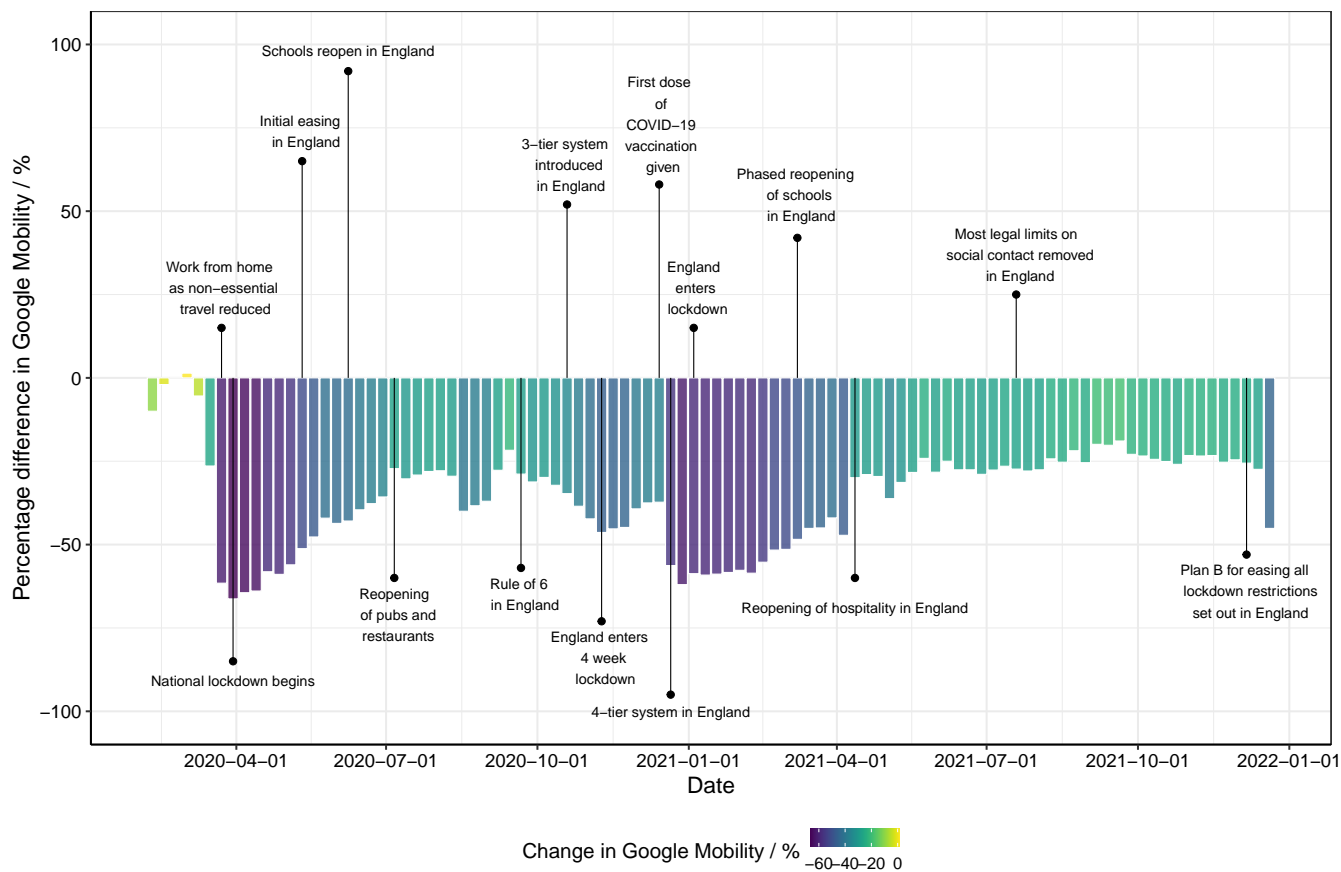
Figure A1. A timeline of COVID restrictions in England from the start of the COVID-19 pandemic until January 2022. Coloured bars represent the weekly change in Google Mobility across the UK.
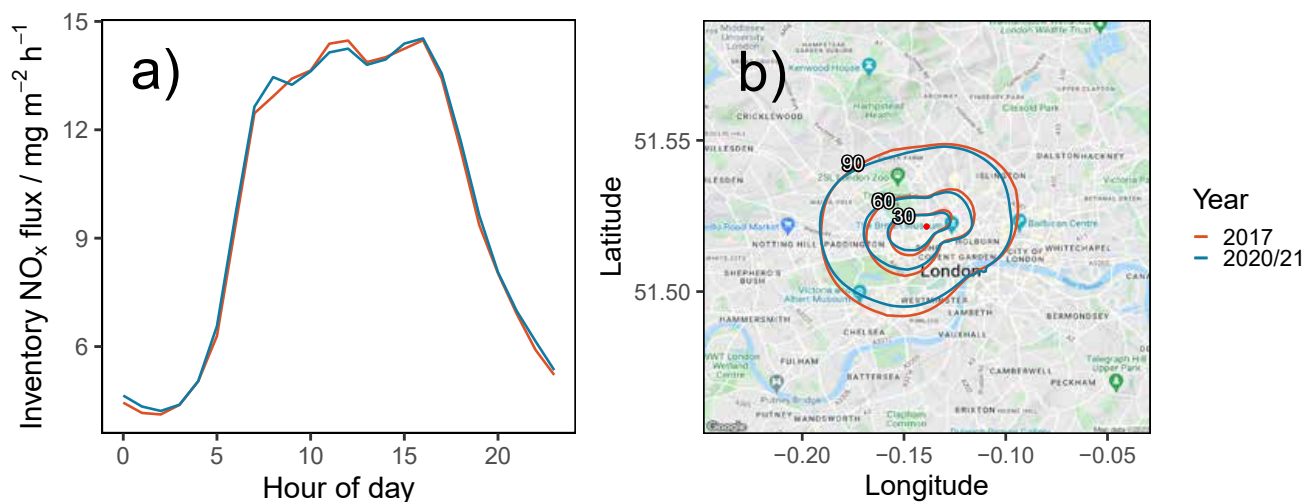
Figure A2. Comparison of a) the diurnal profile of the inventory generated time series and b) the 30, 60 and 90 % footprint contribution contours for the 2017 data set in black and the 2020/21 data set in red. Map in b) produced from Google Maps (© Google Maps 2021) accessed using an API in R.
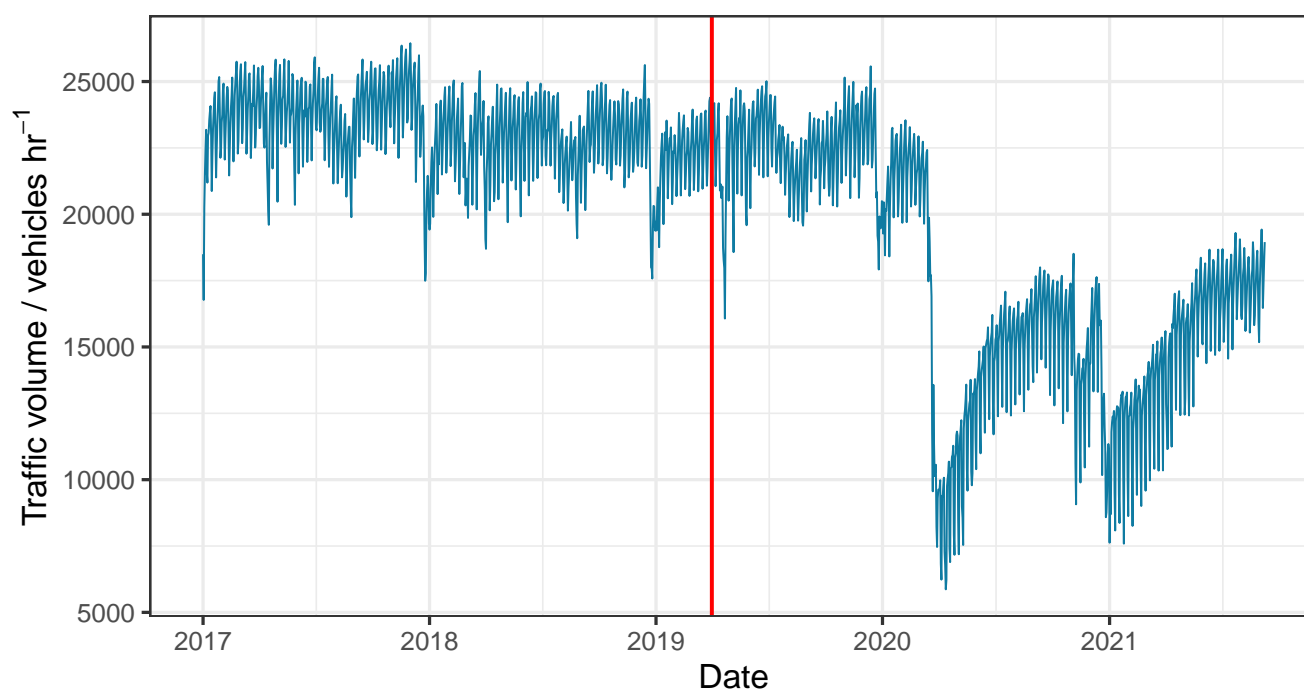
Figure A3. Daily average traffic load from 01/01/2017 - 01/09/2021. The date of the introduction of the ULEZ is marked as a vertical red line.
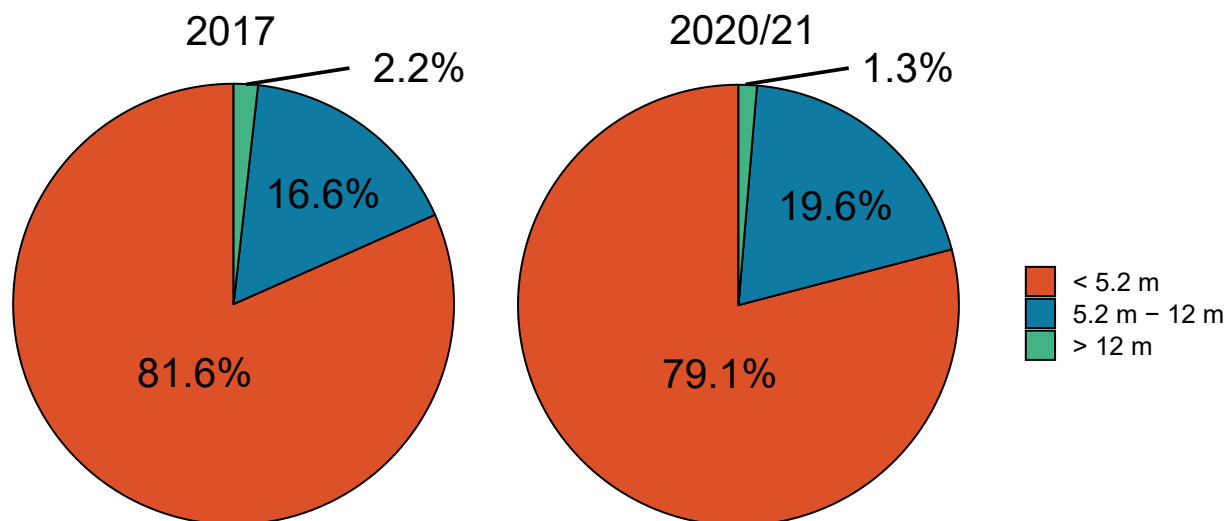
Figure A4. Pie chart for the 2017 and 2020/21 measurement periods displaying the distribution of vehicle length classes measured by the 24 ATC's surrounding the BT Tower.